DOI:
10.1016/j.freeradbiomed.2017.07.007

Document Version
Peer reviewed version

Examining a role for PKG Iα oxidation in the pathogenesis of cardiovascular dysfunction during diet-induced obesity

Olena Rudyk, Philip Eaton

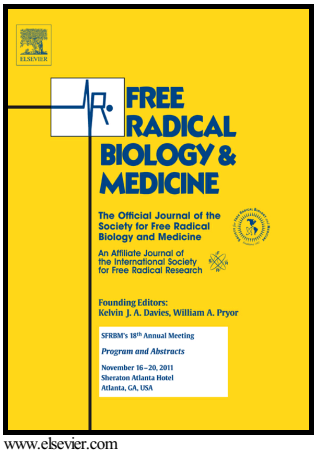

www.elsevier.com

PII: S0891-5849(17)30679-2
DOI: http://dx.doi.org/10.1016/j.freeradbiomed.2017.07.007
Reference: FRB13384

To appear in: *Free Radical Biology and Medicine*

Received date: 17 January 2017
Revised date: 13 June 2017
Accepted date: 5 July 2017

Cite this article as: Olena Rudyk and Philip Eaton, Examining a role for PKG Iα oxidation in the pathogenesis of cardiovascular dysfunction during diet-induced obesity, *Free Radical Biology and Medicine* http://dx.doi.org/10.1016/j.freeradbiomed.2017.07.007

Examining a role for PKG Iα oxidation in the pathogenesis of cardiovascular dysfunction during diet-induced obesity

Olena Rudyk, Philip Eaton*

King's College London, Cardiovascular Division, the British Heart Foundation Centre of Excellence, the Rayne Institute, St Thomas' Hospital, London, SE1 7EH, UK

*Corresponding author. Philip Eaton, Cardiovascular Division, King's College London, The Rayne Institute, 4th Floor, Lambeth Wing, St. Thomas' Hospital, London SE1 7EH, UK. Telephone: 442071880969. Fax: 442071880970. Email: philip.eaton@kcl.ac.uk

Abstract

Background

Protein kinase G (PKG) Iα is the end-effector kinase that mediates nitric oxide (NO)-dependent and oxidant-dependent vasorelaxation to maintain blood pressure during health. A hallmark of cardiovascular disease is attenuated NO production, which in part is caused by NO Synthase (NOS) uncoupling, which in turn increases oxidative stress because of superoxide generation. NOS uncoupling promotes PKG Iα oxidation to the interprotein disulfide state, likely mediated by superoxide-derived hydrogen peroxide, and because the NO-cyclic guanosine monophosphate (cGMP) pathway otherwise negatively regulates oxidation of the kinase to its active disulfide dimeric state. Diet-induced obesity is associated with NOS uncoupling, which may in part contribute to the associated cardiovascular dysfunction due to exacerbated PKG Iα disulfide oxidation to the disulfide state. This is a rational hypothesis because PKG Iα oxidation is known to significantly contribute to heart failure that arises from chronic myocardial oxidative stress.

Methods and Results

Bovine arterial endothelial cells (BAECs) or smooth muscle cells (SMCs) were exposed to drugs that uncouple NOS. These included 1,3-bis(2-chloroethyl)-1-nitrosourea (BCNU) which promotes its S-glutathiolation, 4-diamino-6-hydroxy-pyrimidine (DAHP) which inhibits guanosine-5'-triphosphate-cyclohydrolase 2 to prevent BH_4 synthesis or methotrexate (MTX) which inhibits the regeneration of BH_4 from BH_2 by dihydrofolate reductase. While all the drugs mentioned above induced robust PKG Iα disulfide dimerization in cells, exposure of BAECs to NOS inhibitor L-NMMA did not. Increased PKG Iα disulfide formation occurred in hearts and aortae from mice treated *in vivo* with DAHP (10 mM in a drinking water for 3 weeks). Redox-dead C42S PKG Iα knock-in (KI) mice developed less pronounced cardiac posterior wall hypertrophy and did not develop cardiac dysfunction, assessed by echocardiography, compared to the wild-type (WT) mice after chronic DAHP treatment. WT or KI mice were then subjected to a diet-induced obesity protocol by feeding them with a high fat Western-type diet (RM 60% AFE) for 27 weeks, which increased body mass, adiposity, plasma leptin, resistin and glucagon levels comparably in each genotype. Obesity-induced hypertension, assessed by radiotelemetry, was mild and transient in the WT, while the basally hypertensive KI mice were resistant to further increases in blood pressure increase following high fat feeding. Although the obesogenic diet caused mild cardiac dysfunction in the WT but not the KI mice, gross changes in myocardial structure monitored by echocardiography were not apparent in either genotype. The level of cyclic guanosine monophosphate (cGMP) was decreased in the aortae of WT and KI mice following high fat feeding. PKG Iα oxidation was not evident in the hearts of WT mice fed a high fat diet.

Conclusions

Despite robust evidence for PKG Iα oxidation during NOS uncoupling in cell models, it is unlikely that PKG Iα oxidation occurs to a significant extent *in vivo* during diet-induced obesity and so is unlikely to mediate the associated cardiovascular dysfunction.

Graphical abstract

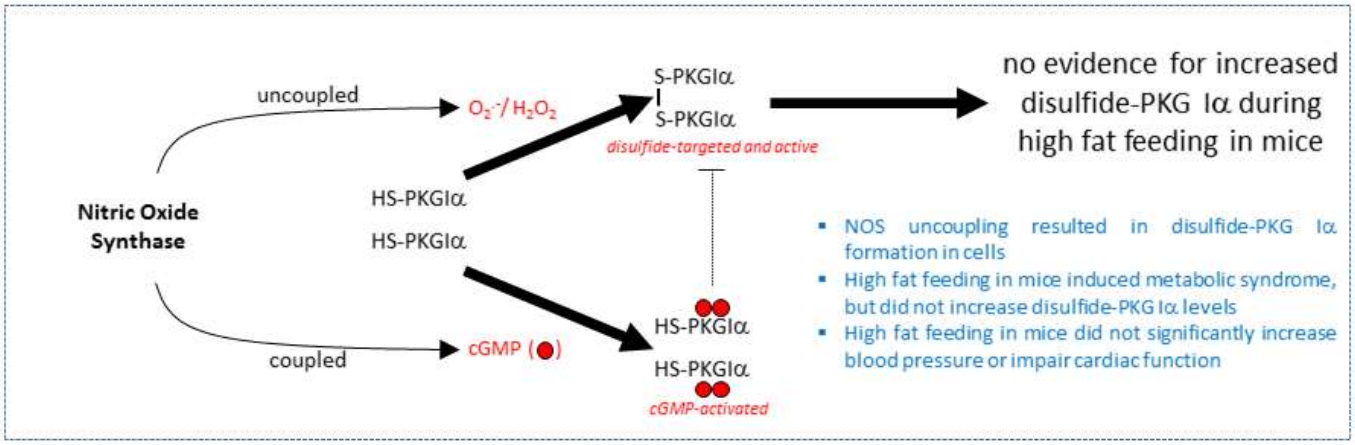

Key words: PKG Iα; disulfide; oxidation; NOS uncoupling; diet-induced obesity

Introduction

A global obesity pandemic, resulting at least in part from altered dietary practices and a decline in physical activity, continues to emerge. Whilst developmental programming and genetic predisposition influence the propensity for obesity [1], a diet high in calories is a major determinant. Obesity is an established risk factor for type-2 diabetes, cancer and cardiovascular diseases [2]. In terms of the cardiovascular system, obesity is associated with atherosclerosis [3], blood vessel dysregulation and hypertension [4], as well as maladaptive changes to the myocardium that alters its structure and compromises its function [5, 6].

Protein kinase G (PKG) is the end-effector kinase that mediates nitric oxide (NO)-dependent vasorelaxation [7], with the Iα isoform mediating oxidant-dependent vasorelaxation to maintain normal healthy blood pressure [8, 9] and regulate diastolic relaxation [10]. Whilst these finding support a role for oxidant-activated PKG Iα in the maintenance of health, oxidation of this kinase have also been observed in the pathogenesis of cardiovascular disease. PKG Iα oxidation contributed to sepsis-induced hypotension [11], as well as myocardial stress-induced apoptosis [12] and cardiac hypertrophy resulting from pressure overload induced by transverse aortic constriction [13]. Consistent with cyclic guanosine monophosphate (cGMP) negatively regulating PKG Iα [14, 15], scenarios in which this second messenger is reduced, such as when NO is less bioavailable, may potentiate oxidation of the kinase to perhaps causatively mediate dysfunction [12]. Consistent with these ideas, pharmacological agents that elevate cGMP or mice expressing C42S PKG Iα that is resistant to disulfide formation [12, 13] demonstrate cardioprotection.

Obesity is associated with endothelial dysfunction, leading to reduced levels of NO and consequentially cGMP, which may causatively manifests as impaired blood vessel relaxation and hypertension [16]. The lower levels of NO is thought to be significantly mediated by ‘uncoupling’ of NO synthase (NOS) resulting from depletion of cofactors such as tetrahydrobiopterin (BH_4) [17]. Such uncoupling is further exacerbated by the concomitant accumulation of BH_2 competing with BH_4 for its NOS binding site, resulting in superoxide production [17, 18]. Dismutation of superoxide to hydrogen peroxide (H_2O_2) can oxidise and so activate PKG Iα via disulfide formation. Consistent with this, obesity results in eNOS uncoupling in mice [19] , and oxidative stress in humans [20]. Oxidative stress can also promote eNOS uncoupling by an additional mechanism involving S-glutathionylation of its reductase domain [21]. Thus NOS uncoupling has a two-fold, synergistic impact on PKG Iα oxidation. This is because uncoupling not only

results in an elevation in oxidants that may target the kinase, but the associated loss of NO will lower cGMP levels that otherwise negatively regulate PKG Iα disulfide formation.

Based on the considerations above, disulfide PKG Iα is likely to occur during times of NOS uncoupling such as obesity, and because of the important roles of this kinase in the cardiovascular system, its oxidation is anticipated to have functional consequences that may or may not be maladaptive. In the current study, we tested the rational hypothesis that potentiated PKG Iα oxidation occurs *in vivo* during scenarios in which NOS is uncoupled such as obesity, utilising a high fat feeding as a model. We also performed complementary investigations using well-established pharmacological agents to monitor oxidation of the kinase in cell, as well as *in vivo*, models. By comparing the response of transgenic knock-in (KI) mice expressing C42S PKG Iα, which is fully resistant to inter-chain disulfide formation at cysteine 42, to wild-type (WT) we sought to define the impact of obesity-induced PKG Iα oxidative activation on cardiovascular function.

2. Materials and Methods

2. 1. Cell experiments and studies with eNOS uncoupling agents in mice

Cells were grown on 12-well plates in an incubator at 37°C with a 95% O_2:5% CO_2 environment. Bovine aortic endothelial cells (BAECs) that are constitutively deficient in PKG Iα were transfected with WT or C42S kinase DNA as described [12]. Once confluent, BAECs and primary rat aortic smooth muscle cells (SMCs) were treated with methotrexate (MTX, Santa Cruz Biotechnology, UK), 1,3-Bis(2-chloroethyl)-1-nitrosourea (BCNU), 2,4-diamino-6-hydroxypyrimidine (DAHP), N^G-monomethyl-L-arginine acetate salt (L-NMMA) or H_2O_2 (all from Sigma, UK) for 3 or 6 hours.

Immunoblotting analysis of the redox state of PKG Iα was performed as described previously [8, 11, 22] with maleimide (100 mM) used in preparation buffers to alkylate thiols and so limit thiol disulfide exchange. Antibodies used in these studies included cGKIα (E-17; Santa Cruz Biotechnology) or PKG antibody (ADI-KAP-PK005; Enzo Life Science). Horseradish peroxidase–linked secondary antibody (Dako) and ECL reagent (GE Healthcare) were used. Digitized immunoblots were analysed quantitatively with a Gel-Pro Analyzer 3.1.

All procedures were performed in accordance with the Home Office Guidance on the Operation of the Animals (Scientific Procedures) Act 1986 in the UK. C42S PKG Iα KI mice constitutively expressing PKG Iα Cys42Ser were generated by Taconic Artemis and maintained on a C56BL/6 as described before [8, 11, 22]. Only male mice were used in the study. In some experiments, age and body-weight matched C56BL/6 male mice were purchased from Charles River, UK. Animals had *ad libitum* access to standard chow and water and were kept in a specific pathogen-free conditions under a 12-hour day/night cycle at 20°C and 60% humidity. DAHP (10 mM) was administered in the drinking water of C57BL/6 mice (n=4/group) for 3 weeks. The water containing DAHP was refreshed every other day. At the end of the protocol, mice were euthanized and hearts and vessels were collected for measurement of the redox status of PKG Iα as described above. In a separate set of experiments C57BL/6 mice were implanted with radiotelemetry transmitters (as described below) and blood pressure was measured for three days to establish the baseline, after which DAHP was administered in the drinking water for a further 3 weeks. In an additional set of experiments, WT or KI mice were given DAHP in their drinking water for 6 weeks, monitoring cardiac function by non-invasive echocardiography, as described below, basally before the drug treatment and then at 1, 3 and 6 weeks afterwards.

2.2. High fat feeding study in mice

Age and body-weight matched WT or KI male mice were employed in this study. WT or KI male mice were fed a control diet of standard chow pellets after weaning (n=10/group) and had *ad libitum* access to water throughout the study. At the age of 10 weeks mice were implanted with radiotelemetry transmitters, as described below, and then kept in individual cages enabling long-term acquisition of telemetric data, as well as accurate measurement of body weight and food intake. After the baseline cardiovascular parameters were recorded, WT or KI mice were chronically administered a control RM3 (Special Diet Services, UK) or high fat (RM 60% AFE, catalogue number 824054, LBS Serving Biotechnology Ltd, UK) diet, on a random basis (n=5/group). This food was provided *ad libitum* in sturdy clear glass 60 ml receptacles with a purpose-drilled hole in the middle of the cap (Suppl. Figure 1), designed to limit

the spillage of food so that consumption could be accurately recorded. The control RM3 diet was ground, so to physically resemble the high fat diet, and was provided in an identical way as the high fat diet, with content of the containers replaced at least twice a week.

The RM 60% AFE diet consisted of 20% protein, 20% carbohydrate and 60% fat, whereas the regular chow RM3 diet comprised 20% protein, 70% carbohydrate and 10% fat. Body weight was recorded weekly for 16 weeks, after which measurements were performed on a fortnightly basis. Food intake was measured randomly at three time points at the beginning, middle or the end of the study. At the end of the feeding protocol, mice were anesthetized and subjected to the terminal non-invasive echocardiographic measurement of their cardiac function as described below. After completion of echocardiography imaging, mice were euthanized and blood was rapidly sampled from the inferior vena cava and immediately analysed for sodium (Na^+), chloride (Cl^-) and blood urea nitrogen (BUN) using an iSTAT blood biochemistry analyser with EC8+ iSTAT cartridges (Abaxis, UK). The remaining blood was centrifuged and the plasma was stored at -80°C until further analysis.

Hearts, aortae and the primary fat depositories were subsequently harvested. The wet mass of the peritoneal, mesenteric, perirenal and epididymal fat tissues was measured to index total body adiposity. The heart and aortic tissue were frozen for subsequent analysis of PKG Iα redox state, as described above.

Plasma content of obesity-related hormones (insulin, glucagon, glucagon-like peptide-1, GLP-1, resistin, ghrelin, gastric inhibitory polypeptide, GIP) and adipokines (leptin and plasminogen activator inhibitor-1, PAI-1) was measured using a suspension bead array immunoassay kit following the manufacturer's instructions (Bio-Plex Pro Mouse Diabetes Assay, Bio-Rad) using a Bio-Plex MAGPIX Multiplex Reader (Bio-Rad). In addition, the amount of cGMP content was measured in plasma and aortae, using an Biotrak Enzyme immunoassay (RPN226, GE Healthcare) as before [12]. Briefly, aortae were snap-frozen and homogenized in cold 6% trichloroacetic acid on ice. Aliquots were centrifuged at 2000 g for 15 min at 4 °C, and the pellet was discarded. The supernatant was washed 4 times with five volumes of water-saturated diethyl ether. The remaining aqueous extract was lyophilized and then dissolved in the manufacturer's assay buffer prior to analysis following the acetylation EIA procedure as outlined in the manufacturer's instructions. Plasma was diluted (1:10) in the manufacturer's assay buffer prior to analysis following their instructions.

Telemetric measurements

Blood pressure, heart rate (HR) and locomotor activity were assessed by invasive radiotelemetry in conscious freely moving mice as before [8, 11, 22]. In brief, mice were anesthetised with 2% isoflurane (Centaur Services) in 0.5 l of oxygen per minute with peri-operative analgesia (methadone, 1 mg/kg of body mass, Comfortan, Dechra, UK). A TA11PA-C10 probe catheter (Data Science International, St Pauls, MN, USA) was implanted into the aortic arch via the left carotid artery. Following 7 days of recovery, mice were placed above the telemetric receivers and the blood pressure, HR and locomotor activity was recorded by scheduled sampling for 10 second every 5 minutes. In each telemetry study baseline data was collected for 3 days before the interventions. During the high fat feeding study, the telemetry data was acquired each weekend for the first 16 weeks, after which is it was collected fortnightly until week 23 when the battering the probes expired.

Echocardiography

Telemetered (high fat feeding study) or non-telemetered (DAHP study) mice were anesthetised with 2% isoflurane in 0.5 l of oxygen per minute and examined by echocardiography using a non-invasive high resolution Vevo 770 echocardiography system (RMV707B, VisualSonics, Toronto, ON, Canada) with a RMV-707B transducer running at 30 MHz. The core body temperature was maintained at 37°C with a feedback-regulated body temperature probe. High resolution, two-dimensional B-mode and M-mode images were obtained at the level of the papillary muscles and further analyzed offline with Vevo Software (VisualSonics) as before [11].

3. Results and Discussion

Uncoupling of NOS *in vitro* causes PKG Iα disulfide dimerization

The effect of NOS uncoupling on PKG Iα disulfide dimerization was tested in cell culture studies. BCNU treatment caused PKG Iα disulfide dimerization in both cultured bovine aortic endothelial cells (BAECs) transfected with WT PKG Iα construct (Figure 1A) and rat aortic smooth muscle cells (SMCs) (Figure 1B). This is consistent with BCNU being an inhibitor of glutathione reductase, which could lead to elevated glutathione disulfide with consequent uncoupling by causing S-glutathiolation of NOS [21, 23] via a disulfide exchange reaction. However it should be considered that BCNU, also known as carmustine, has limited selectivity [24], which is consistent with its being a small di-alkylating agent that will react promiscuously with many protein thiols it encounters. Thus, it is difficult to be confident of the precise mechanism by which PKG Iα oxidation may have occurred after exposure to BCNU.

DAHP also induced PKG Iα disulfide dimerization in BAECs and SMCs (Figure 1A-B), consistent with its activity as a GTP cyclohydrolase I inhibitor [25]. GTP cyclohydrolase I mediates *de novo* synthesis of BH_4, which when limited uncouples NOS so that it instead of NO, generates superoxide. The latter then dismutates to H_2O_2, which in turn can oxidise PKG Iα. MTX, which inhibits the regeneration of BH_4 from BH_2 by dihydrofolate reductase [26, 27], and so also uncouples NOS, similarly caused PKG Iα oxidation. MTX-induced oxidation was only observed in the endothelial but not the smooth muscle cells (Figure 1, A-B), with the underlying reason for this discrepancy being unclear. Exposure of BAECs to L-NMMA did not increase PKG Iα disulfide dimerization (Figure 1A), which it may have been anticipated to by inhibiting NOS and so reducing the abundance of NO and cGMP. As cGMP negatively regulates the oxidation of PKG Iα [12, 14] L-NMMA may lead to accumulation of the disulfide form of the kinase. However, as inhibitors of NOS may also limit superoxide and so H_2O_2 production [18], such interventions may also limit a key mechanism of PKG Iα oxidative activation and explain the lack of an effect by L-NMMA.

C42S PKG Iα KI mice are protected from a moderate cardiac dysfunction induced by eNOS uncoupling

Since robust PKG Iα oxidation was observed after *in vitro* treatment of BAECs or SMCs with DAHP, and taking into account studies reported by others [25, 28], this compound was selected for use in follow-up *in vivo* studies. Mice were chronically administered DAHP in their drinking water for 3 weeks, which induced oxidation of PKG Iα in their hearts and aortae as anticipated (Figure 2A). In contrast, we did not observe similar increases in kinase oxidation in the mesenteric resistance vessels from the same animals (Figure 2A). Although this result is in consistent with the lack of acute or chronic alteration in mean arterial pressure (MAP) that was observed (Suppl. Figure 2), it contrasts with previous observations in rats, in which DAHP increased blood pressure acutely to generate a sustained hypertension [28]. DAHP also increased blood pressure in FVB mice [25], and again although the reason a lack of an effect in our studies is unclear, we note that our C57BL/6 mice are a different strain. Blood pressure is mediated by the tone of resistance blood vessels, and as such, it is notable that DAHP failed to induce oxidation in mesenteries. The reason why PKG Iα oxidation was observed in the aorta and heart, but not in mesenteries is unclear, especially as then kinase is more susceptible to oxidation in the smaller vessels [14]. Although mesenteries are widely used in investigations of blood vessel regulation, it is important to consider that as part of the splanchnic vascular bed that their contribution to peripheral resistance is minimal. Furthermore, these vessels are also significantly regulated by cyclic adenosine monophosphate and protein kinase A, a signalling pathway that has not been assessed in this study. Whilst it would be valuable to determine the redox state of PKG Iα in other blood vessels relevant to peripheral resistance, such as skeletal muscle arterioles, this is difficult to achieve for technical reasons. Dissection and preparation of these small vessels takes much longer than isolation of the aorta or heart, making the redox state measurements of PKG Iα in such tissues unreliable. Another consideration regarding the lack of an effect of DAHP on a blood pressure is that uncoupled NOS enzymes are thought to be a source of H_2O_2 basally in resistance blood vessels and that it is this, and not NO, that principally mediates blood vessel relaxation [29]. In this scenario, in which H_2O_2 is thought to significantly mediate the endothelium-derived hyperpolarization factor-dependent mechanism of vasodilation that is a major mechanism of vasodilation in resistance vessels and for blood pressure regulation [29-31], perhaps hypertension is not rationally anticipated as a result of NOS uncoupling.

Although DAHP had no impact on PKG Iα oxidation in mesenteric blood vessels, it was effective in inducing this change in the heart where this event may have direct effects on myocardial function or structure, despite the lack of an effect on blood pressure. Consequently, we then treated WT or KI mice with DAHP and compared their cardiac structure and function non-invasively using echocardiography, serially over 6 weeks (Figure 2B). Cardiac output gradually declined to ~21% and the diastolic posterior wall thickness increased by ~47% by the end of the 6-week protocol in WT mice. In contrast, the KI mice showed no decline in their cardiac output and developed only a small increase (~12%) in the cardiac posterior wall thickness by the end of the protocol. These differential functional changes between genotypes were also matched by serial, time-dependent changes in cardiac mass measured by

echocardiography. These analyses showed that the C42S PKG Iα KI mice were resistant to cardiac hypertrophy compared to WT, which was further corroborated by measurement of the wet mass of the heart isolated (normalised to tibia length) at the end of the protocol (Figure 2C). Cardiac hypertrophy can result from hypertension, but as mentioned above, DAHP did not increase blood pressure in these studies and so therefore cannot underlie the hypertrophic growth of the myocardium, which was attenuated in the KI. Consistent with our observation that cardiac PKG Iα becomes oxidised upon exposure to DAHP, this compound depressed myocardial function, which was also apparent when isolated ventricular myocytes were studied [25]. However, as DAHP also increased blood pressure in that study [25], direct effects on myocardial cells or those secondary to hypertension cannot be distinguished [25]. In this connection, it is notable that pressure overload resulting from transverse aortic constriction increased PKG Iα oxidation [13], as did exposure to doxorubicin [12] and that in each of these studies the C42S PKGIα KI mice were significantly resistant to myocardial structural and functional alterations induced by the intervention in WT mice. A logical implication for these findings is that disulfide PKG Iα formation in the heart is maladaptive, and this may be in part because it contributes to stress-induced apoptosis [12], or prevents interaction with the transient receptor potential channel 6 which can mediate ant-hypertrophic signalling [13].

Obesity, PKG Iα oxidation and cardiovascular dysfunction

WT or KI mice were fed either a normal or a high fat obesogenic diet for 27 weeks. The obesogenic diet progressively increased the mass of the mice over time compared to those on a normal diet (Figure 3A). Indeed, this increase in mass was comparable between genotypes, as measured at the final 27-week time point (Figure 3B). Food intake was also similar between genotypes, albeit as anticipated mice consumed less of the highly calorific high fat food compared to the normal chow (Figure 3C). Total body adiposity was estimated as a sum of peritoneal, mesenteric, peri-renal and epididymal wet fat mass after 27 weeks of either diet and compared between genotypes (Figure 4A). There was a similar increase in total body fat after 27 weeks of high fat feeding in WT and KI mice (Figure 4B-C); although there is an insignificant trend towards exacerbated adiposity in the KI mice fed a normal diet. Overall, it was evident that the high fat diet induced obesity in the mice as expected. It is of note that transgenic mice overexpressing PKG I exposed to a high fat diet for 16 weeks were resistant to mass and adiposity gain, although this only occurred in females but not in male mice [32].

Blood pressure, HR and activity were compared in WT and KI mice using radiotelemetry over the 23 weeks of high fat feeding (Figure 5A-C). Monitoring for a longer duration was precluded by the expiration of the battery in the telemetric probes. A moderate but transient MAP increase was observed in the WT mice peaking around 6, 10 and 23 weeks of the high fat diet protocol (Figure 5A). Analysis of the average MAP over the 23 weeks revealed that there was a trend for this to be higher in the WT mice fed a high fat diet compared to the KI (Figure 5D), although this just failed to reach significance at the 5% level ($p=0.08$). KI mice were basally hypertensive compared to the WT whilst on a normal diet (Suppl. Figure 3), consistent with earlier studies [8, 22]. However, when KI mice were switched to the high fat diet their blood pressure did not increase, indicating a differential response compared to the WT (Figure 5D). The average HR decline was similar in both WT and KI mice fed a normal diet over the 23-week period, possibly due to an active baroreflex function serving to buffer blood pressure increases caused by age. This decrease in HR was less prominent with the high fat feeding, although no differences were observed between the WT and the KI mice. Analysis of the average locomotor activity over the 23 weeks revealed a strong trend toward a sedimentary life-style associated with obesity; notably there was a more pronounced decrease in activity in the KI mice fed a high fat diet compared to the WT mice.

At the end of the 27 weeks of high fat feeding the structure and the function of the heart was assessed by echocardiography (Figure 6A-B). There was a trend towards a lower stroke volume and cardiac output in the KI compared with the WT mice fed a normal diet. Although it failed to reach significance, this is in line with the previously published data for younger mice [8, 12]. KI mice fed a normal diet had smaller left ventricular diastolic dimension and volume than the WT mice on a normal diet, consistent with the diastolic dysfunction observed in the KI mice previously [8, 10]. The obesogenic high fat diet caused both systolic and diastolic dysfunction in the WT mice (Figure 6B) which agrees with other studies [6] and could result from a mild hypertension observed in the WT mice. Such cardiac dysfunction was not observed in the KI (Figure 6B); again, in line with the lack of hypertensive response to high fat feeding in the KI mice. The plasma levels of Na^+, Cl^- and blood urea nitrogen (BUN) were increased in the WT mice fed a high fat diet, but not in the KI mice (Figure 6C), which may represent mild renal dysfunction in the transgenic. Such dysfunction might explain why MAP increased by 8.0±2.6 mmHg in the high fat fed WT mice, whilst it only increased by 1.8±0.4 mmHg in the KIs (Figure 5D). The less pronounced changes in the

KI mice are perhaps due to their smaller pressor response than in the WT. A trend towards higher BUN in the KI fed a normal diet could be age-related, although we previously reported similar renal function in healthy young (12-weeks old) WT and KI mice [8].

The amounts of leptin, resistin and glucagon in plasma were robustly increased in both WT and KI mice fed a high fat diet (Suppl. Figure 4) compared to the animals consuming a normal diet. An increase in ghrelin and GIP was only observed in the plasma of WT mice fed a high fat diet, while GLP-1 was only increased in the plasma of high fat fed KI mice. There was a strong trend towards an increased level of insulin and PAI-1in the plasma of both genotypes (Suppl. Figure 4). Consistent with this, albeit insignificant, trend towards higher basal adiposity in the KI mice (Figure 4), we also observed increased plasma ghrelin, insulin, resistin, glucagon and GIP in the KI compared with the WT mice fed a normal diet. Taken together, these data are in accordance with studies showing metabolic syndrome can be induced in mice on a high fat diet [33]. Although plasma lipid profiling was not performed, it is envisaged that the higher body mass and increased adiposity in mice with a high fat diet, together with their elevated circulating leptin levels would likely be associated with accumulation of triglycerides, often characteristic of metabolic syndrome [33].

The plasma levels of cGMP were not altered in WT or KI mice following high fat feeding; however, there was a decrease of cGMP level in the aortae of WT and KI mice fed a high fat diet, compared to those fed a normal diet (Suppl. Figure 5). This is consistent with NOS uncoupling in the vasculature following high fat feeding. eNOS uncoupling was previously reported in vessels from obese db/db mice with features of type 2 diabetes [34], as well as in perivascular adipose tissue of mice fed a high fat diet [19]. However, the loss of cGMP is not a conclusive evidence of NOS uncoupling, as other mechanisms, such as phosphodiesterase 5 activation or soluble guanylate cyclase inhibition, could also decrease the production cGMP. For example, modulation of the soluble guanylate cyclase redox state can alter its activity resulting in perturbations of cGMP levels in the vasculature [35].

The level of PKG Iα disulfide dimer was similar in the hearts of WT mice fed either normal or a high fat diet (Figure 6D). This was unexpected, because of the previous observation of increased PKG Iα oxidation and moderate functional and structural cardiac changes in a model of chronic NOS uncoupling with DAHP. Although our measurement of the redox state of PKG Iα was made at the end of the protocol after 27 weeks of high fat feeding, it is plausible that earlier sampling may have yielded different results. Lack of PKG Iα oxidation following high fat feeding in the heart tissues is not in agreement with the reduced level of cGMP in the vasculature, although it was not possible to perform complementary measurements of PKG Iα disulfide dimerisation in the aortae. There is a complex relationship between cGMP and oxidation of PKG Iα. Whilst cGMP binding attenuates inter-disulfide formation [14], how this oxidation potentially modulates cyclic nucleotide binding remains unclear. Although significant crystallographic information is available for PKG [36-38], the structural impact of cGMP binding or oxidation on the holoenzyme remains to be elucidated. Protein expression levels of antioxidant enzymes superoxide dismutase (SOD) 1, 2 and 3 in the hearts were not altered following high fat feeding in either genotype. Interestingly, the levels of hyperoxidised (sulfinated or sulfonated) peroxiredoxin protein were increased in the hearts of WT, but not KI, mice fed a high fat diet. Hyperoxidised DJ-1 was not altered in either genotype on either of the two diets (Suppl. Figure 6).

Whilst mice exposed to high fat feeding clearly developed metabolic syndrome-like symptoms, the impact on the cardiovascular system in terms of hypertension or impaired cardiac performance was negligible. This was unexpected, as hypertension has been observed with a similar high fat feeding model in mice [39]. Of note, a high fat diet impaired cardiac contractility in *Drosophila* [40] and mice [41]. The lack of the cardiac structural changes after high fat feeding agrees with the lack of increased PKG Iα disulfide dimerization in the hearts of WT mice on a high fat diet. Perhaps a more severe dietary insult, such as prolonged high fat feeding combined with high sucrose or fructose, might have resulted in a more pronounced biochemical and cardiovascular phenotypical alterations. In addition, we cannot rule out a potential contribution of the adenylate cyclase-cyclic adenosine monophosphate-protein kinase A pathway which could be differentially modulated in the *in vivo* models we employed.

In summary, we observed robust PKG Iα oxidation in vascular cells treated with drugs that uncouple NOS. Uncoupling of NOS *in vivo* also induced PKG Iα oxidation in aorta and hearts and was associated with moderate cardiac structural and functional abnormalities in WT mice, with the KIs being protected from such changes. These observations are in line with previous studies reporting an injurious role for PKG Iα disulfide dimerization in the setting of chronic myocardial oxidative stress. In contrast, there was no evidence of PKG Iα oxidation in the hearts of the WT mice chronically exposed to a high fat diet. We conclude that despite robust *in vitro* evidence of PKG Iα

disulfide dimerization under conditions of NOS uncoupling treatments, it is likely that oxidation of this kinase plays a neutral role in cardiovascular adaptation triggered by a diet-induced obesity.

Acknowledgements

Dr Olena Rudyk is a British Heart Foundation Intermediate Basic Science Research Fellow. This work was supported by a British Heart Foundation Programme grant awarded to Philip Eaton, the Medical Research Council and the Department of Health via the NIHR cBRC award to Guy's & St Thomas' NHS Foundation Trust. We thank Dr. Oleksandra Prysyazhna for her enormous help with breeding C42S PKGIα KI mouse colony. We also thank Dr Adam Greenstein for providing the RM 60% AFE high fat diet for pilot experiments.

References

[1] Popkin, B. M.; Adair, L. S.; Ng, S. W. Global nutrition transition and the pandemic of obesity in developing countries. *Nutrition reviews* **70:**3-21; 2012.

[2] Zhang, C.; Rexrode, K. M.; van Dam, R. M.; Li, T. Y.; Hu, F. B. Abdominal obesity and the risk of all-cause, cardiovascular, and cancer mortality: sixteen years of follow-up in US women. *Circulation* **117:**1658-1667; 2008.

[3] Gomez-Hernandez, A.; Beneit, N.; Diaz-Castroverde, S.; Escribano, O. Differential Role of Adipose Tissues in Obesity and Related Metabolic and Vascular Complications. *International journal of endocrinology* **2016:**1216783; 2016.

[4] Ahmad, F. S.; Ning, H.; Rich, J. D.; Yancy, C. W.; Lloyd-Jones, D. M.; Wilkins, J. T. Hypertension, Obesity, Diabetes, and Heart Failure-Free Survival: The Cardiovascular Disease Lifetime Risk Pooling Project. *JACC. Heart failure* **4:**911-919; 2016.

[5] Lavie, C. J.; Milani, R. V.; Ventura, H. O. Obesity and cardiovascular disease: risk factor, paradox, and impact of weight loss. *Journal of the American College of Cardiology* **53:**1925-1932; 2009.

[6] Alpert, M. A.; Omran, J.; Bostick, B. P. Effects of Obesity on Cardiovascular Hemodynamics, Cardiac Morphology, and Ventricular Function. *Current obesity reports* **5:**424-434; 2016.

[7] Francis, S. H.; Busch, J. L.; Corbin, J. D.; Sibley, D. cGMP-dependent protein kinases and cGMP phosphodiesterases in nitric oxide and cGMP action. *Pharmacological reviews* **62:**525-563; 2010.

[8] Prysyazhna, O.; Rudyk, O.; Eaton, P. Single atom substitution in mouse protein kinase G eliminates oxidant sensing to cause hypertension. *Nature medicine*: 2012.

[9] Burgoyne, J. R.; Madhani, M.; Cuello, F.; Charles, R. L.; Brennan, J. P.; Schroder, E.; Browning, D. D.; Eaton, P. Cysteine redox sensor in PKGIa enables oxidant-induced activation. *Science* **317:**1393-1397; 2007.

[10] Scotcher, J.; Prysyazhna, O.; Boguslavskyi, A.; Kistamas, K.; Hadgraft, N.; Martin, E. D.; Worthington, J.; Rudyk, O.; Rodriguez Cutillas, P.; Cuello, F.; Shattock, M. J.; Marber, M. S.; Conte, M. R.; Greenstein, A.; Greensmith, D. J.; Venetucci, L.; Timms, J. F.; Eaton, P. Disulfide-activated protein kinase G Ialpha regulates cardiac diastolic relaxation and fine-tunes the Frank-Starling response. *Nature communications* **7:**13187; 2016.

[11] Rudyk, O.; Phinikaridou, A.; Prysyazhna, O.; Burgoyne, J. R.; Botnar, R. M.; Eaton, P. Protein kinase G oxidation is a major cause of injury during sepsis. *Proceedings of the National Academy of Sciences of the United States of America* **110:**9909-9913; 2013.

[12] Prysyazhna, O.; Burgoyne, J. R.; Scotcher, J.; Grover, S.; Kass, D.; Eaton, P. Phosphodiesterase 5 Inhibition Limits Doxorubicin-induced Heart Failure by Attenuating Protein Kinase G Ialpha Oxidation. *J Biol Chem* **291:**17427-17436; 2016.

[13] Nakamura, T.; Ranek, M. J.; Lee, D. I.; Shalkey Hahn, V.; Kim, C.; Eaton, P.; Kass, D. A. Prevention of PKG1alpha oxidation augments cardioprotection in the stressed heart. *The Journal of clinical investigation* **125:**2468-2472; 2015.

[14] Burgoyne, J. R.; Prysyazhna, O.; Rudyk, O.; Eaton, P. cGMP-Dependent Activation of Protein Kinase G Precludes Disulfide Activation: Implications for Blood Pressure Control. *Hypertension* **60:**1301-1308; 2012.

[15] Muller, P. M.; Gnugge, R.; Dhayade, S.; Thunemann, M.; Krippeit-Drews, P.; Drews, G.; Feil, R. H2O2 lowers the cytosolic Ca2+ concentration via activation of cGMP-dependent protein kinase I alpha. *Free Radical Bio Med* **53:**1574-1583; 2012.

[16] Sansbury, B. E.; Hill, B. G. Regulation of obesity and insulin resistance by nitric oxide. *Free radical biology & medicine* **73:**383-399; 2014.

[17] Bendall, J. K.; Douglas, G.; McNeill, E.; Channon, K. M.; Crabtree, M. J. Tetrahydrobiopterin in cardiovascular health and disease. *Antioxidants & redox signaling* **20:**3040-3077; 2014.
[18] Xia, Y.; Tsai, A. L.; Berka, V.; Zweier, J. L. Superoxide generation from endothelial nitric-oxide synthase - A Ca2+/calmodulin-dependent and tetrahydrobiopterin regulatory process. *Journal of Biological Chemistry* **273:**25804-25808; 1998.
[19] Xia, N.; Horke, S.; Habermeier, A.; Closs, E. I.; Reifenberg, G.; Gericke, A.; Mikhed, Y.; Munzel, T.; Daiber, A.; Forstermann, U.; Li, H. G. Uncoupling of Endothelial Nitric Oxide Synthase in Perivascular Adipose Tissue of Diet-Induced Obese Mice. *Arterioscl Throm Vas* **36:**78-85; 2016.
[20] Vincent, H. K.; Taylor, A. G. Biomarkers and potential mechanisms of obesity-induced oxidant stress in humans. *International journal of obesity* **30:**400-418; 2006.
[21] Chen, C. A.; Wang, T. Y.; Varadharaj, S.; Reyes, L. A.; Hemann, C.; Talukder, M. A.; Chen, Y. R.; Druhan, L. J.; Zweier, J. L. S-glutathionylation uncouples eNOS and regulates its cellular and vascular function. *Nature* **468:**1115-1118; 2010.
[22] Rudyk, O.; Prysyazhna, O.; Burgoyne, J. R.; Eaton, P. Nitroglycerin fails to lower blood pressure in redox-dead Cys42Ser PKG1alpha knock-in mouse. *Circulation* **126:**287-295; 2012.
[23] Crabtree, M. J.; Brixey, R.; Batchelor, H.; Hale, A. B.; Channon, K. M. Integrated redox sensor and effector functions for tetrahydrobiopterin- and glutathionylation-dependent endothelial nitric-oxide synthase uncoupling. *The Journal of biological chemistry* **288:**561-569; 2013.
[24] Maker, H. S.; Weiss, C.; Brannan, T. S. The Effects of Bcnu (1,3-Bis(2-Chloroethyl)-1-Nitrosourea) and Ccnu (1-(2-Chloroethyl)-3-Cyclohexyl-1-Nitrosourea) on Glutathione-Reductase and Other Enzymes in Mouse-Tissue. *Res Commun Chem Path* **40:**355-366; 1983.
[25] Ceylan-Isik, A. F.; Guo, K. K.; Carlson, E. C.; Privratsky, J. R.; Liao, S. J.; Cai, L.; Chen, A. F.; Ren, J. Metallothionein abrogates GTP cyclohydrolase I inhibition-induced cardiac contractile and morphological defects: role of mitochondrial biogenesis. *Hypertension* **53:**1023-1031; 2009.
[26] Crabtree, M. J.; Tatham, A. L.; Hale, A. B.; Alp, N. J.; Channon, K. M. Critical role for tetrahydrobiopterin recycling by dihydrofolate reductase in regulation of endothelial nitric-oxide synthase coupling: relative importance of the de novo biopterin synthesis versus salvage pathways. *The Journal of biological chemistry* **284:**28128-28136; 2009.
[27] Crabtree, M. J.; Hale, A. B.; Channon, K. M. Dihydrofolate reductase protects endothelial nitric oxide synthase from uncoupling in tetrahydrobiopterin deficiency. *Free radical biology & medicine* **50:**1639-1646; 2011.
[28] Mitchell, B. M.; Dorrance, A. M.; Webb, R. C. Phenylalanine improves dilation and blood pressure in GTP cyclohydrolase inhibition-induced hypertensive rats. *Journal of cardiovascular pharmacology* **43:**758-763; 2004.
[29] Shimokawa, H. Hydrogen peroxide as an endothelium-derived hyperpolarizing factor. *Pflug Arch Eur J Phy* **459:**915-922; 2010.
[30] Shimokawa, H.; Matoba, T.; Nakashima, M.; Hirakawa, Y.; Mukai, Y.; Hirano, K.; Kanaide, H.; Takeshita, A. Identification of hydrogen peroxide as an endothelium-derived hyperpolarizing factor in mice. *Edhf 2000***:**249-258; 2001.
[31] Shimokawa, H.; Matoba, T. Hydrogen peroxide as an endothelium-derived hyperpolarizing factor. *Pharmacol Res* **49:**543-549; 2004.
[32] Nikolic, D. M.; Li, Y. Z.; Liu, S.; Wang, S. X. Overexpression of Constitutively Active PKG-I Protects Female, But Not Male Mice From Diet-Induced Obesity. *Obesity* **19:**784-791; 2011.
[33] Wong, S. K.; Chin, K. Y.; Suhaimi, F. H.; Fairus, A.; Ima-Nirwana, S. Animal models of metabolic syndrome: a review. *Nutrition & metabolism* **13:**65; 2016.
[34] Youn, J. Y.; Zhou, J.; Cai, H. Bone Morphogenic Protein 4 Mediates NOX1-Dependent eNOS Uncoupling, Endothelial Dysfunction, and COX2 Induction in Type 2 Diabetes Mellitus. *Mol Endocrinol* **29:**1123-1133; 2015.
[35] Zheng, X. X.; Ying, L.; Liu, J.; Dou, D.; He, Q.; Leung, S. W. S.; Man, R. Y. K.; Vanhoutte, P. M.; Gao, Y. S. Role of sulfhydryl-dependent dimerization of soluble guanylyl cyclase in relaxation of porcine coronary artery to nitric oxide. *Cardiovascular research* **90:**565-572; 2011.
[36] Qin, L. Y.; Reger, A. S.; Guo, E.; Yang, M. P.; Zwart, P.; Casteel, D. E.; Kim, C. Structures of cGMP-Dependent Protein Kinase (PKG) I alpha Leucine Zippers Reveal an Interchain Disulfide Bond Important for Dimer Stability. *Biochemistry* **54:**4419-4422; 2015.
[37] Kim, J. J.; Lorenz, R.; Arold, S. T.; Reger, A. S.; Sankaran, B.; Casteel, D. E.; Herberg, F. W.; Kim, C. Crystal Structure of PKG I:cGMP Complex Reveals a cGMP-Mediated Dimeric Interface that Facilitates cGMP-Induced Activation. *Structure* **24:**710-720; 2016.

[38] Osborne, B. W.; Wu, J.; McFarland, C. J.; Nickl, C. K.; Sankaran, B.; Casteel, D. E.; Woods, V. L.; Kornev, A. P.; Taylor, S. S.; Dostmann, W. R. Crystal Structure of cGMP-Dependent Protein Kinase Reveals Novel Site of Interchain Communication. *Structure* **19:**1317-1327; 2011.
[39] Chaar, L. J.; Coelho, A.; Silva, N. M.; Festuccia, W. L.; Antunes, V. R. High-fat diet-induced hypertension and autonomic imbalance are associated with an upregulation of CART in the dorsomedial hypothalamus of mice. *Physiological reports* **4**; 2016.
[40] Birse, R. T.; Choi, J.; Reardon, K.; Rodriguez, J.; Graham, S.; Diop, S.; Ocorr, K.; Bodmer, R.; Oldham, S. High-fat-diet-induced obesity and heart dysfunction are regulated by the TOR pathway in Drosophila. *Cell metabolism* **12:**533-544; 2010.
[41] Calligaris, S. D.; Lecanda, M.; Solis, F.; Ezquer, M.; Gutierrez, J.; Brandan, E.; Leiva, A.; Sobrevia, L.; Conget, P. Mice Long-Term High-Fat Diet Feeding Recapitulates Human Cardiovascular Alterations: An Animal Model to Study the Early Phases of Diabetic Cardiomyopathy. *PloS one* **8**; 2013.

Figure 1. *In vitro* treatment of cells with NOS-uncoupling drugs results in robust PKG Iα disulfide dimerization. (A) Bovine aortic endothelial cells (BAECs) treatment with BCNU, MTX or DAHP (100 μM for 3 hours) resulted in significant increase of PKG Iα disulfide dimerisation, whereas treatment with L-NMMA (100 μM for 3 hours) did not. **(B)** Smooth muscle cells (SMCs) treatment with BCNU or DAHP (100 μM for 6 hours) resulted in significant increase of PKG Iα disulfide dimerisation, whereas treatment with methotrexate (100 μM for 6 hours) did not. A positive control, namely 100 μM H_2O_2 for 30 min, causes nearly all PKG Iα to disulfide dimerise. n=6-8/group. Data represented as mean±SEM. *P≤0.05, **P≤0.01 versus vehicle treatment.

Figure 2. *In vivo* treatment with DAHP causes PKG Iα disulfide dimerization and adaptive cardiac structural and functional abnormalities. (**A**) Increase of PKG Iα disulfide dimerization in heart or aorta, but not in mesenteric vessels from mice treated with DAHP (10 mM in the drinking water for 3 weeks). (**B**) Heart mass to tibia length ratio was lower in the KI mice compared to WT after 6 weeks of treatment with DAHP. (**C**) Time-dependent changes in left ventricular (LV) mass, stroke volume, cardiac output and posterior wall thickness at the baseline and during 1, 3 and 6 weeks of DAHP treatment in WT and KI mice. n=6/group. Data represented as mean±SEM. *P≤0.05, versus vehicle treatment (A) or versus KI (B and C). nd – normal diet, od – obesogenic high fat det.

Figure 3. High fat feeding results in similar body weight gain and food intake in WT and KI mice. (**A**) Changes in body mass during 27 weeks of control or obesogenic diet in WT or KI mice (**B**) Higher body mass and similar heart mass in the WT or KI mice after 27 weeks of feeding with high fat obesogenic diet (grey bars) versus normal diet (white bars). (**C**) Food intake measured at the beginning, middle and before the end of the experiment in WT and KI mice fed a control (white bars) or an obesogenic diet (grey bars). n=5/group. Data represented as mean±SEM. *P≤0.05 versus normal diet.). nd – normal diet, od – obesogenic high fat det.

Figure 4. High fat feeding has a similar effect on adiposity in WT and KI mice. (A) Mesenteric, perirenal and epididymal fat to body weight ratio are significantly increased after 27 weeks of feeding with obesogenic diet (grey bars) versus mice fed a normal diet (white bars); (B) total body fat and (C) total fat to body weight ratio are similarly increased in WT and KI mice after 27 weeks on obesogenic diet. n=5/group. Data represented as mean±SEM. *P≤0.05, **P≤0.01, ***P≤0.001 versus normal diet; #P≤0.05 versus WT.). nd – normal diet, od – obesogenic high fat det.

Figure 5. High fat feeding has a mild effect on blood pressure. (**A-C**) Mean Arterial Pressure (MAP), Heart Rate (HR) and locomotor Activity changes in WT and KI mice fed with a normal diet (white marker types) or an obesogenic (grey marker types) diet for 23 weeks. (**D**) Delta response in MAP, HR and Activity in WT and KI mice after feeding with obesogenic diet (grey bars) for 27 weeks, compared to the normal diet (white bars). n=5/group. Data represented as mean±SEM. *P≤0.05 versus normal diet.). nd – normal diet, od – obesogenic high fat det.

Figure 6. High fat feeding has no effect of PKG Iα disulfide dimerisation. (**A**) Similar left ventricular (LV) mass, stroke volume, cardiac output and posterior wall thickness in WT and KI mice after feeding with obesogenic diet (grey bars) for 27 weeks. (**B**) Smaller LV systolic and diastolic dimension and volume in WT mice fed an obesogenic diet, compared to the KI. (**C**) Blood concentration of sodium (Na^+), chloride (Cl^-) and blood urea nitrogen (BUN) in WT and KI mice after feeding with obesogenic diet (grey bars) for 27 weeks, compared to the normal diet (white bars). (**D**) Feeding mice with high fat obesogenic diet for 27 weeks did not result in increase of PKG Iα disulfide dimerization in heart. n=5/group. Data represented as mean±SEM. *P≤0.05 versus normal diet.). nd – normal diet, od – obesogenic high fat det.

Supplementary Figure 1. Top - Photographic capture of sturdy clear glass 60 ml receptacles with a purpose-drilled hole in the cap to provide food in a high fat feeding study**. Bottom** - Composition of the normal and the high fat diets according to the information provided by the supplier.

Supplementary Figure 2. *In vivo* treatment with DAHP does not cause acute or chronic hypertension in C57BL/6 mice. n=4/group. Data represented as mean±SEM.

Supplementary Figure 3. KI mice develop hypertension, compared to the WT mice. n=10/group. Data represented as mean±SEM. *P≤0.05, **P≤0.01 versus WT.

Supplementary Figure 4. Hormonal profile in plasma from WT or KI mice following a high fat or normal diet. n=5/group. Data represented as mean±SEM. *P≤0.05, **P≤0.01, ***P≤0.001 versus obesogenic diet. #P≤0.05 versus WT. GIP, gastric inhibitory polypeptide; GLP-1, glucagon-like peptide-1; PAI-1, plasminogen activator inhibitor-1.

Supplementary Figure 5. cGMP profile in plasma and aortae of WT or KI mice following a high fat or normal diet. n=3-5/group. Data represented as mean±SEM. **P≤0.01 versus obesogenic diet. cGMP, cyclic guanosine monophosphate; SNP, sodium nitroprusside.; Veh –Vehicle.

Supplementary Figure 6. Expression of antioxidant enzymes and markers of oxidation in hearts from WT or KI mice following a high fat or normal diet. n=5/group. Data represented as mean±SEM. **P≤0.01 versus obesogenic diet. #P≤0.05 versus WT. SOD-1-3, superoxide dismutase; GAPDH, glyceraldehyde 3-phosphate dehydrogenase; PRX-SO_3, hyperoxidised peroxiredoxin; DJ-1-SO_3, hyperoxidised protein deglycase (Parkinson disease protein 7).

Highlights

- NOS uncoupling resulted in disulfide-PKG Iα formation in cells
- High fat feeding in mice induced metabolic syndrome, but did not increase disulfide-PKG Iα levels
- High fat feeding did not significantly increase blood pressure or impair cardiac function in wild-type or C42S PKG Iα knock-in transgenic mice

Figure 1.

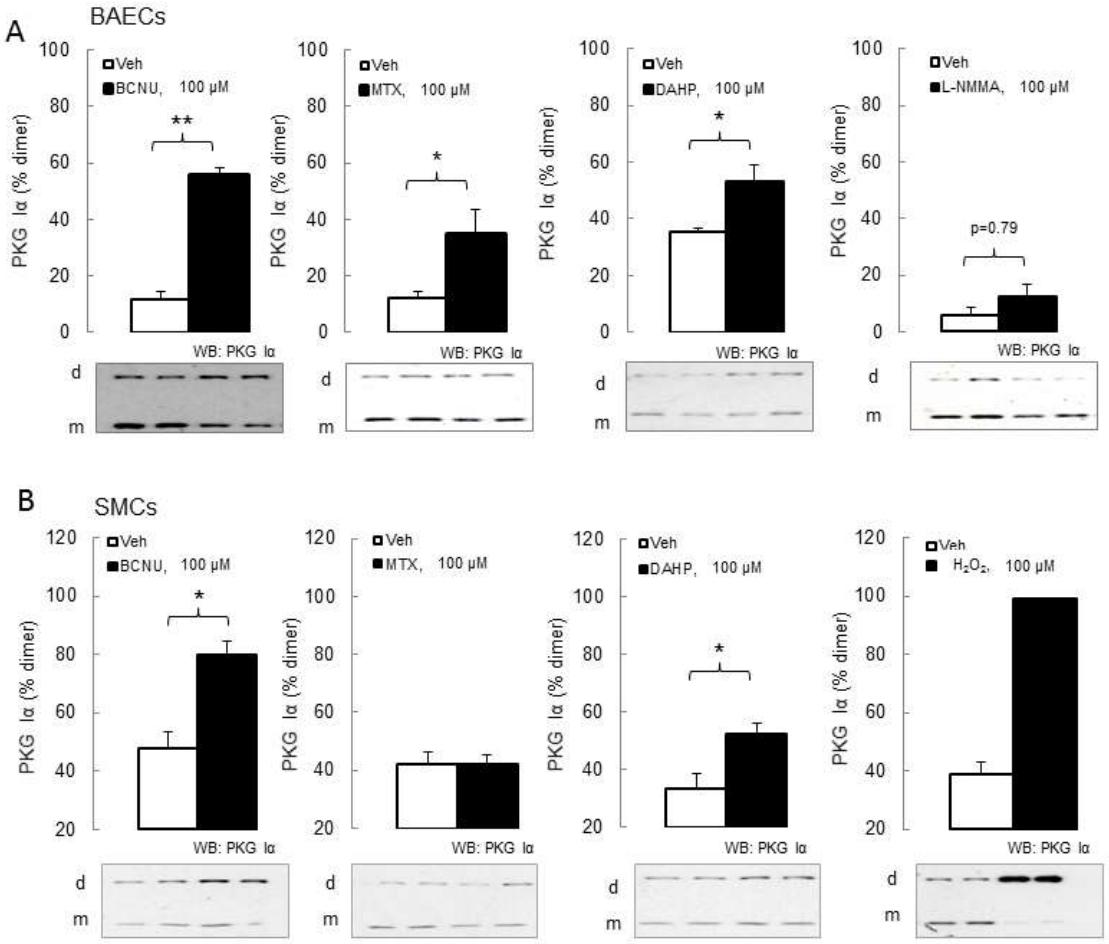

Figure 2.

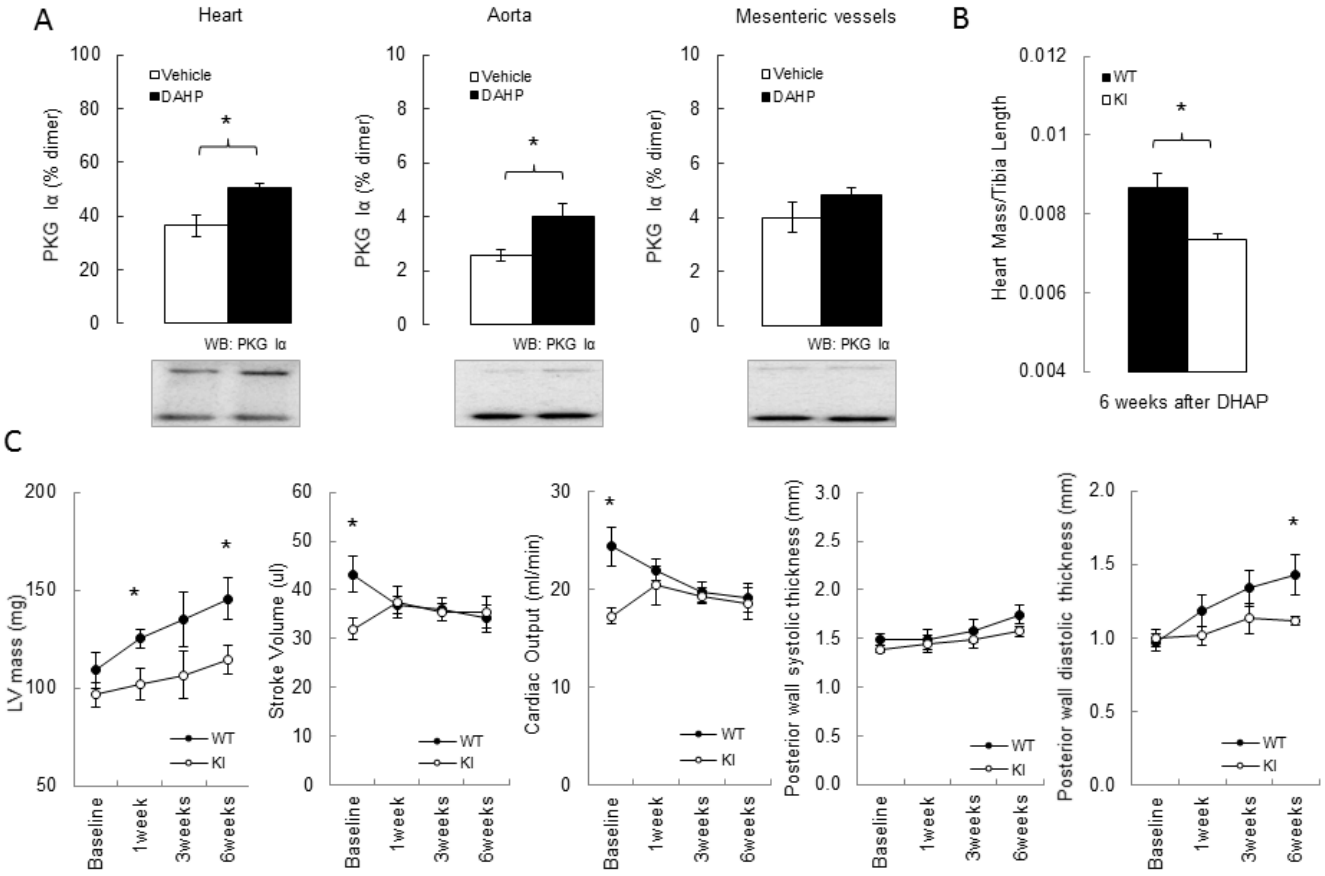

Figure 3.

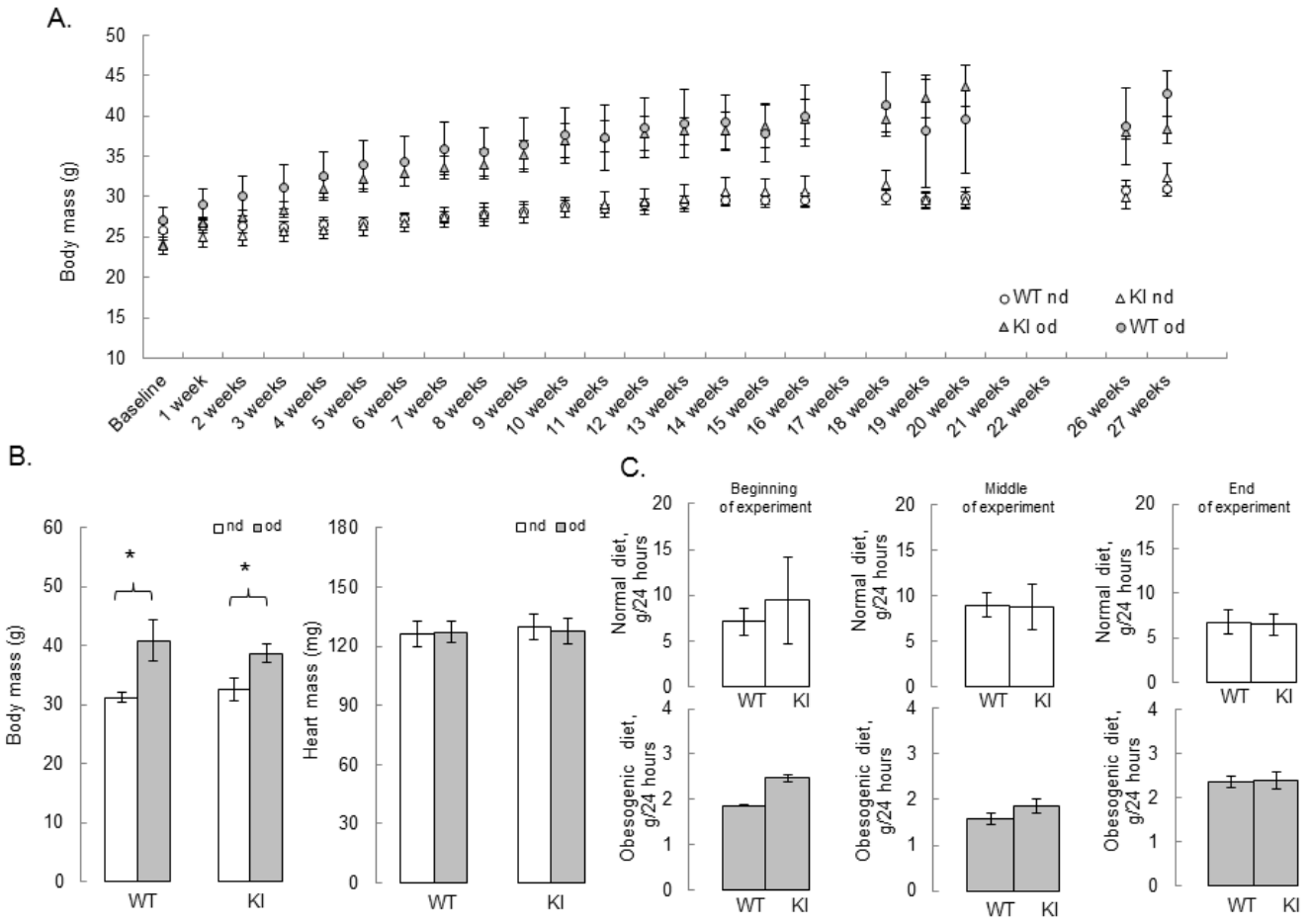

Figure 4.

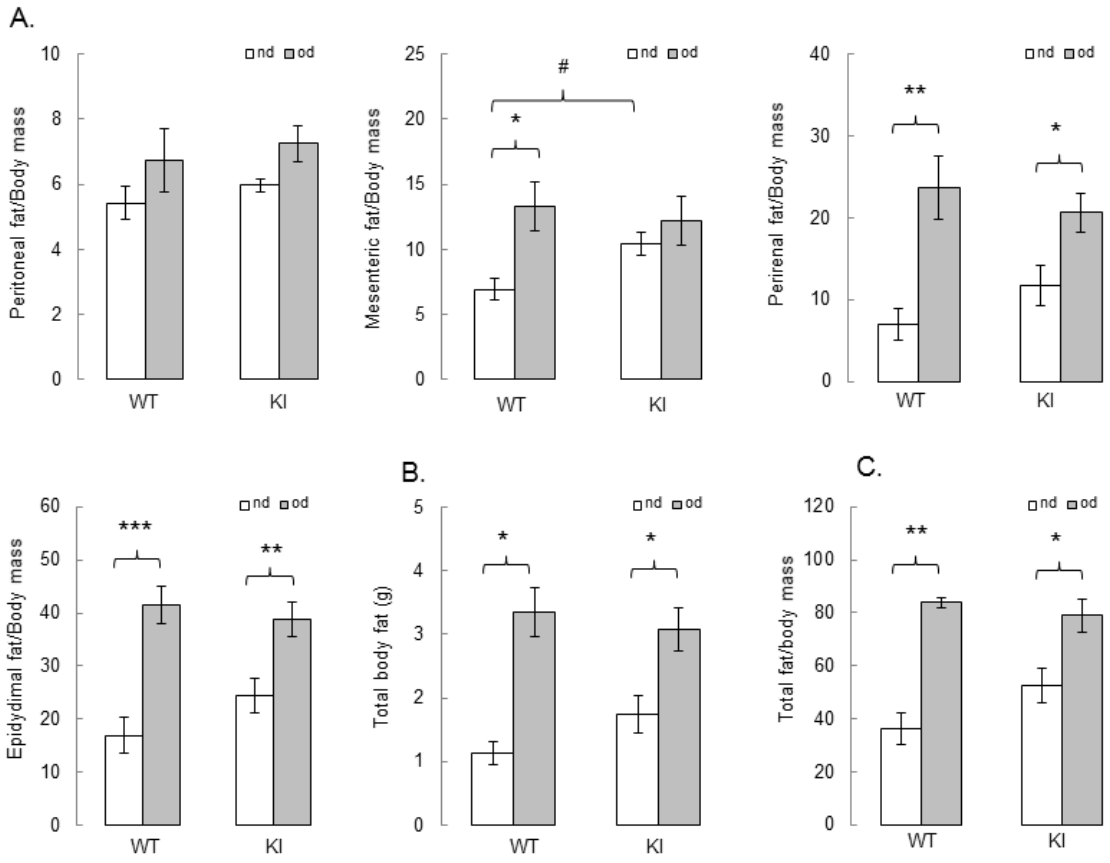

Figure 5.

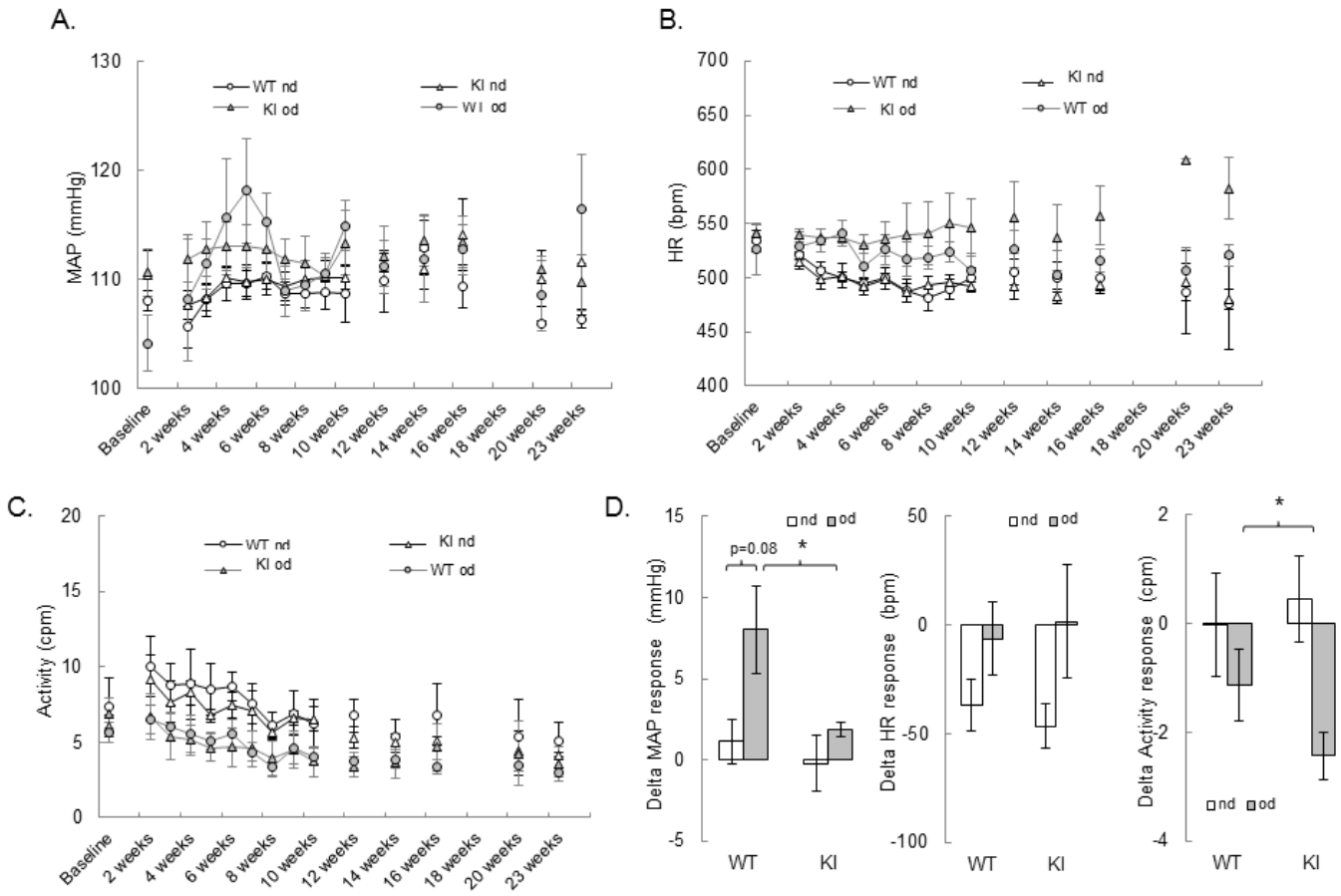

Figure 6.